ISSN 1063-7850, Technical Physics Letters, 2019, Vol. 45, No. 5, pp. 485–488. © Pleiades Publishing, Ltd., 2019.
Russian Text © The Author(s), 2019, published in Pis'ma v Zhurnal Tekhnicheskoi Fiziki, 2019, Vol. 45, No. 10, pp. 13–16.

A Highly Selective Bandpass Filter Based on Suspended Substrate Resonators with a Two-Sided Stripline Pattern

B. A. Belyaev[a,b]*, A. M. Serzhantov[b], Ya. F. Bal'va[a], An. A. Leksikov[a], and E. O. Grushevskii[a]

[a] *Kirensky Institute of Physics, Siberian Branch, Russian Academy of Sciences, Krasnoyarsk, 660036 Russia*

[b] *Siberian Federal University, Krasnoyarsk, 660074 Russia*

**e-mail: belyaev@iph.krasn.ru*

Received January 15, 2019; revised January 15, 2019; accepted February 20, 2019

Abstract—New resonator design employing a hairpin stripline conductor with a stub situated on one side of a dielectric substrate and regular stripline conductors (connected to a screen) on the other side. Eigenfrequencies of the first three oscillation modes of this resonator can be made closer to each other, so that the resonances of two modes are involved in the formation of the passband while the third mode resonance forms a minimum of the transmission coefficient adjacent to the passband. A structure comprising four resonators of this type has the characteristic of an eighth-order bandpass filter arranged in a case with 45 × 16 × 6.25-mm internal dimensions possessing $f_0 = 0.52$ GHz central frequency with a 14% relative bandwidth. The filter is highly selective due to the attenuation poles being close to the pass band and a wide high-frequency stopband extending above a fivefold f_0 value at a level of -100 dB.

DOI: 10.1134/S1063785019050225

It is well known that microwave bandpass filters are among the most important elements of modern systems of communications, radiolocation, radio navigation, and special measurement instrumentation [1, 2]. These filters in many cases determine the design and, more importantly, the performance of radio engineering equipment that directly depends on the frequency-selective characteristics of filters. Requirements for the characteristics of filters—in particular, to their cutoff attenuation rates, magnitudes, and bandwidths—are continuously increasing. This stimulates the creation of new filters with miniature design and high selectivity as an important and topical task.

Filters designed on the basis of microstripe or stripline resonators on suspended substrates are some of the smallest devices [1–3]. As a rule, the frequency response passband cutoff rates for any filter design are increased by using filters of higher orders with greater number of resonators [4], additional stub elements [5], or multimode resonators [6]. The latter approach allows the filter order to be increased without increasing the number of resonators and enhances attenuation in the stopbands. However, the width of the high-frequency stopband (limited by the resonances of higher oscillation modes forming parasitic passbands) is frequently increased using filters with dissimilar (stepped impedance) resonators [7–9] based on quasi-lumped elements manufactured on suspended substrates [10] or by so-called "LTCC technology" [11, 12].

One of the most effective approaches to filter design, capable of simultaneously expanding the high-frequency stopband, increasing the degree of attenuation, and reducing the dimensions of planar bandpass filters, consists in using multiconductor stripline resonators [13, 14]. However, the frequency response characteristics of these filters have no attenuation poles providing increase in the frequency response slope (cutoff attenuation rate), which allows the filter selectivity to be improved only by increasing the number of resonators. It is an additional drawback that the process of filter manufacturing based on multiconductor stripline resonators is rather complicated and requires using special advanced technology equipment.

The present work was aimed at studying a multistripline filter based on a new miniature stripline resonator design with two-sided pattern of conductors on a suspended substrate (Fig. 1a). In this scheme, the resonator arranged in metal case *5* is formed by hairpin stripe conductor *2* connected at the center to stub *3* situated on one side of substrate *1*. The opposite substrate side bears regular stripe conductors *4* shorted at one end to the screen, which are positioned strictly against open ends of the stripline structure on the first side, have the corresponding width, and form quasi-lumped capacitors significantly reducing the resonator size. Input and output ports with 50-Ω impedance are connected to transmission lines *6*.

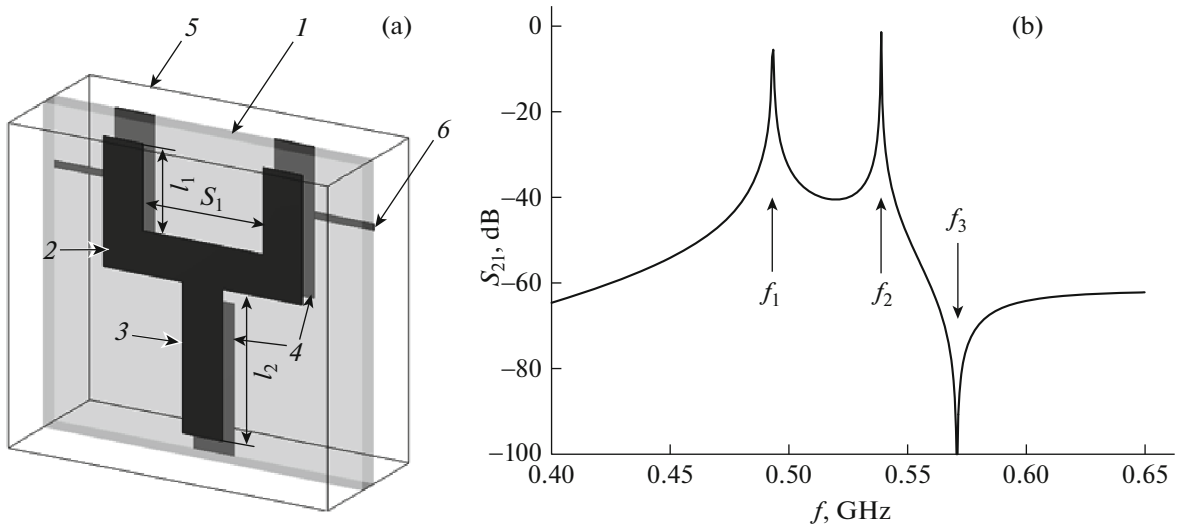

Fig. 1. (a) Schematic diagram of a stripline resonator: (*1*) suspended dielectric substrate, (*2*) hairpin stripe conductor, (*3*) stub, (*4*) regular stripe conductors, (*5*) metal case, and (*6*) transmission lines for input/output port connections. (b) Frequency response of the resonator weakly coupled to the input and output ports.

Figure 1b shows the frequency response of the proposed resonator as calculated using a 3D electrodynamic model analysis in CST-Microwave Studio program package in the case of a resonator structure weakly coupled to the input and output ports. The resonator structure parameters were as follows: 0.25-mm-thick plate of TBNS high-frequency ceramics with relative dielectric constant $\varepsilon = 80$; screen to substrate surface distance, 3 mm; stripe conductor width, 1 mm; and filter structure dimensions $l_1 = 5.9$ mm, $l_2 = 7.0$ mm, and $S_1 = 6.0$ mm (Fig. 1a) and the free ends of hairpin stripe and stub conductors spaced from the substrate edge by 0.5 mm. Investigations showed that the resonator is three-mode with close eigenfrequencies f_1, f_2, and f_3. Note that the resonances of two modes at frequencies f_1 and f_2 are involved in formation of the filter passband, while the third mode resonance at frequency f_3 forms an attenuation pole near the passband. It is also important to note that, by selecting the resonator stub length, the value of f_3 can be varied so as to set the attenuation pole either on the left or right side of the passband, thus increasing the frequency response slope on the corresponding side.

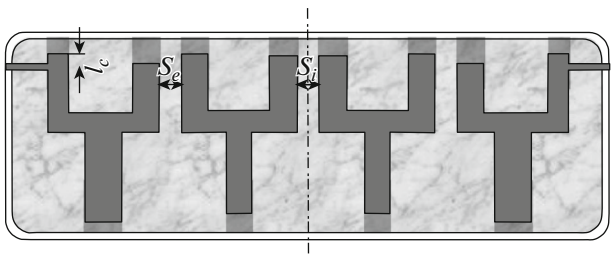

Fig. 2. Topology of stripline conductors in the four-resonator bandpass filter.

Figure 2 shows the topology of stripe conductors in a four-resonator bandpass filter structure on 0.25-mm-thick suspended substrate with $\varepsilon = 80$, S_e gaps between stripe conductors in the external pairs, and S_i gaps between stripe conductors in the internal pairs. The upper and lower screens were spaced by 3 mm from the substrate surface. It should be noted that the given four-resonator bandpass filter design based on stripline hairpin resonators with stubs have 12 oscillation modes with close eigenfrequencies (three modes of each resonator). The resonances of eight modes form the filter passband, while resonances of the other four modes form attenuation poles on the left and right near the passband. For this reason, the frequency response slopes of this filter are much steeper than those for the filter based on eight hairpin resonators without stub elements.

The proposed filter was tuned by means of the "manual" parametric synthesis using a 3D electrodynamic model analysis in the CST-Microwave Studio program package. The central frequency of the filter passband was tuned by selecting dimensions of the hairpin stripe resonators and the corresponding stripe conductors on the opposite substrate side, closed with one end on the screen. The passband width was tuned by varying S_e and S_i gaps between resonators. The points of conductive connection of the segments of lines connecting terminal resonators to the ports were shifted by l_c relative to the end of the external hairpin conductor (Fig. 2), which allowed the preset level of microwave power reflection losses in the passband to be tuned. The lengths of stubs and corresponding stripe conductors on the opposite substrate side were

varied to tune the frequencies of attenuation poles so that they occurred on the right and left of the passband, thus ensuring highly steep fronts and nearly symmetric shape of the frequency response curve.

For certainty, we have synthesized a bandpass filter for the communication channel with passband central frequency $f_0 = 0.52$ GHz at a relative width of $f/f_0 = 14\%$ measured on a 3-dB level of minimum losses and a −14-dB level of microwave power reflected from the input. Figure 3 shows frequency responses of (dashed line) the synthesized filter and (solid line) the experimental prototype manufactured in accordance with the structural parameters determined by synthesis. This prototype (shown without an upper lid in Fig. 3) had a dielectric substrate with dimensions of 16 × 45 mm.

As can be seen, the frequency responses of the proposed filter show a quite good agreement of theory and experiment. The passband central frequency of the experimental prototype almost coincides with the calculated value, while the relative passband width even turned out to be somewhat smaller (by ~0.5%) than the result of calculation. It should also be noted that the minimum losses of experimental prototype measured in the filter passband were only 0.4 dB above the calculated level and amounted to ~1.9 dB.

The proposed filter design demonstrates both a wide high-frequency stopband (extending to frequencies above $5f_0$ at a −100-dB level) and high slope of the frequency response. The filter prototype presented in Fig. 3 has approximately equal slopes of both low-frequency ($K_l = 4.1$) and high-frequency ($K_h = 4.0$) passband front attenuation rates as calculated by the following formulas [4]:

$$K_l = \frac{\Delta f_3/2}{\Delta f_l - \Delta f_3/2}, \quad K_h = \frac{\Delta f_3/2}{\Delta f_h - \Delta f_3/2}, \qquad (1)$$

where Δf_3 is the filter passband width at a level of −3 dB and Δf_l and Δf_h are passband widths measured from central frequency f_0 to the low-frequency (f_l) and high-frequency (f_h) passband fronts at a level of −30 dB of minimum losses. Evidently, the equality of K_l and K_h values is indicative of a symmetric shape of the frequency response of the synthesized filter. However, it is also important to note another useful feature of the proposed filter design, which allows creating filters with asymmetric frequency responses by significantly increasing the slope of one front. For this purpose, it is sufficient to select stub stripe lengths so as to place all attenuation poles on the corresponding side of the frequency response curve.

It should also be noted that the width of the high-frequency stopband in the proposed filter increases with decreasing thickness of the dielectric substrate, which is accompanied by simultaneous reduction in the length of resonators and, hence, in overall dimensions of the entire filter. The extension of the high-frequency stopband also grows but to a lower degree with increasing width of stripe conductors and larger distance from the suspended substrate surfaces to screens.

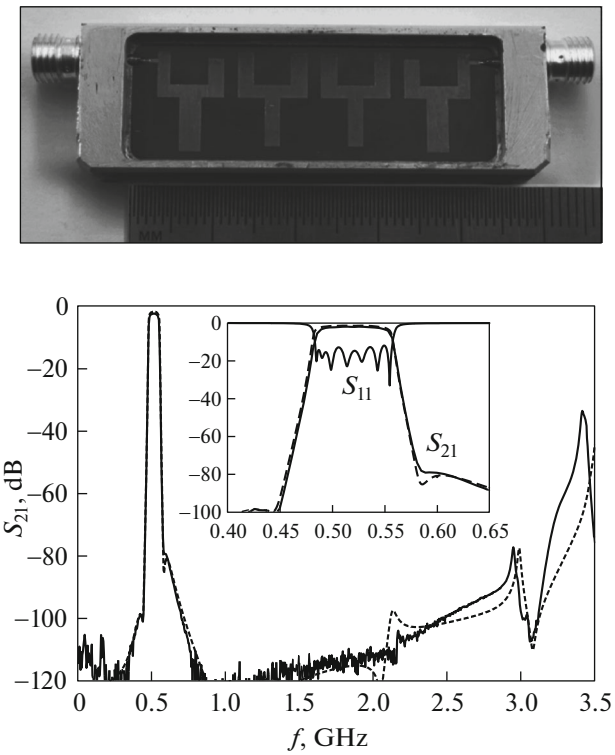

Fig. 3. Measured (solid lines) and simulated (dashed lines) frequency dependences of reflection losses S_{11} and transmission losses S_{21} of the proposed filter model. The top inset shows a photograph of the prototype filter (without an upper lid).

FUNDING

This study was supported in part by the Ministry of Education and Science of the Russian Federation, agreement no. 14.575.21.0142, unique project identifier RFMEFI57517X0142.

REFERENCES

1. I. C. Hunter, *Theory and Design of Microwave Filters*, Vol. 48 of *IET Electromagnetic Waves Series* (Cambridge Univ. Press, Cambridge, 2006).
2. M. A. Morgan, *Reflectionless Filters* (Artech House Microwave Library, Boston, London, 2017).
3. J.-S. Hong, *Microstrip Filters for RF/Microwave Applications* (Wiley, Hoboken, 2011).
4. B. A. Belyaev, A. A. Leksikov, and V. V. Tyurnev, J. Commun. Technol. Electron. **49**, 1228 (2004).
5. A. A. Aleksandrovsky, B. A. Belyaev, and A. A. Leksikov, J. Commun. Technol. Electron. **48**, 358 (2003).

6. B. A. Belyaev, S. A. Khodenkov, An. A. Leksikov, and V. F. Shabanov, Dokl. Phys. **62**, 289 (2017).
7. X. B. Wei, Y. Shi, P. Wang, J. X. Liao, Z. Q. Xu, and B. C. Yang, J. Electromagn. Waves Appl. **26**, 1095 (2012).
8. J.-T. Kuo and E. Shih, IEEE Trans. Microwave Theory Technol. **51**, 1554 (2003).
9. S.-C. Lin, P.-H. Deng, Y.-S. Lin, C.-H. Wang, and C. H. Chen, IEEE Trans. Microwave Theory Technol. **54**, 1011 (2006).
10. B. A. Belyaev, A. S. Voloshin, A. S. Bulavchuk, and R. G. Galeev, Tech. Phys. Lett. **42**, 622 (2016).
11. D. V. Kholodnyak, V. M. Turgaliev, I. V. Munina, P. A. Tural'chuk, and I. B. Vendik, Radiotekhnika, No. 7, 132 (2012).
12. A. Simin, D. Kholodnyak, and I. Vendik, Kompon. Tekhnol., No. 5, 190 (2005).
13. B. A. Belyaev, A. M. Serzhantov, V. V. Tyurnev, Y. F. Balva, and A. A. Leksikov, Prog. Electromagn. Res. C **48**, 37 (2014).
14. B. A. Belyaev, A. M. Serzhantov, A. A. Leksikov, Y. F. Balva, and A. A. Leksikov, Microwave Opt. Technol. Lett. **59**, 2212 (2017).

Translated by P. Pozdeev